Sustainable Conversion of Mixed Plastics into Porous Carbon Nanosheets with High Performances in Uptake of Carbon Dioxide and Storage of Hydrogen

Jiang Gong,[†,‡] Beata Michalkiewicz,[§] Xuecheng Chen,*[,†,§] Ewa Mijowska,[§] Jie Liu,[†] Zhiwei Jiang,[†] Xin Wen,[†] and Tao Tang*[,†]

[†]State Key Laboratory of Polymer Physics and Chemistry, Changchun Institute of Applied Chemistry, Chinese Academy of Sciences, Changchun 130022, China

[‡]University of Chinese Academy of Sciences, Beijing 100049, China

[§]Institute of Chemical and Environment Engineering, West Pomeranian University of Technology, Szczecinul. Pulaskiego 10, 70-322 Szczecin, Poland

Ⓢ *Supporting Information*

ABSTRACT: Conversion of waste plastics into high value-added carbon nanomaterials has gained wide research interest due to the requirement of sustainable development and the ever-increasing generation of waste plastics. However, most of studies are limited to single component plastic; besides, little attention has been paid to carbon nanosheets (CNS). Herein, CNS were prepared by catalytic carbonization of mixed plastics consisting of polypropylene, polyethylene, polystyrene, poly-(ethylene terephthalate), and polyvinyl chloride on organically modified montmorillonite. After KOH activation, porous CNS (PCNS) were produced. The morphology, microstructure, phase structure, textural property, surface element composition, and thermal stability of PCNS were investigated. PCNS contained randomly oriented lattice fringes and showed a layered morphology consisting of thin, leaf-like, agglomerated nanosheets ranging from hundreds of nanometers to several micrometers in length. Besides, PCNS exhibited high specific surface area (1734 m^2/g) and large pore volume (2.441 cm^3/g). More importantly, PCNS displayed high performances in the uptake of carbon dioxide and storage of hydrogen. It is believed that this work not only paves the way for utilization of mixed waste plastics but also provides a facile sustainable approach for the large-scale production of valuable PCNS for energy storage and environmental remediation.

KEYWORDS: *Mixed plastics, Sustainable approach, Porous carbon nanosheet, Carbon dioxide, Hydrogen*
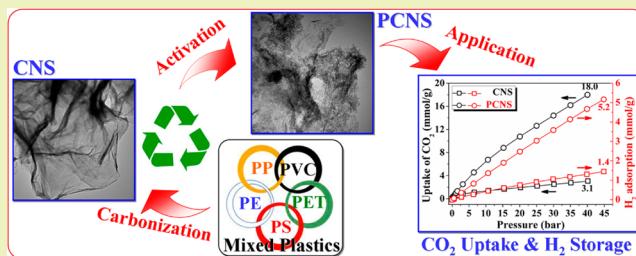
INTRODUCTION

The intensive consumption of fossil fuels and growing environmental concerns observed in the recent decades are bringing world attention to the importance of exploiting sustainable production of fuels, chemicals, and materials,[1−7] and minimizing contaminations including greenhouse gas emissions[8,9] and disposal of solid wastes.[10−13] Waste plastics are among the largest and most problematic sources of wastes. It was reported that the world production of plastics increased from 1.7 million tons in 1950 to 288 million tons in 2012,[14] and about 32.6 million tons of waste plastics were correspondingly generated in United States.[15] Traditional methods for the treatment of waste plastics are landfill and incineration, which are far from being widely accepted due to their related environmental pollution. Apparently, the recovery of waste plastics and conversion of them into high value-added materials are crucial to advance the effective utilization of waste plastics because most of them are not biodegradable and have a long life. Mechanical recycling of waste plastics is limited by the low quality of the recycled plastic mixture. Chemical recycling can recover the petrochemical components from waste plastics to produce useful monomers, fuels, gases, and other chemicals.[16−19] However, the development of facile, economically viable, and sustainable approaches to transform waste plastics into valuable products still remains a great challenge.

Because most of plastics mainly consist of the carbon element, extensive studies have been conducted to reutilize waste plastics to synthesize high value-added carbon nanomaterials (CNMs). Up to now, great progress[20−40] has been made on the conversion of plastics, including polypropylene (PP), polyethylene (PE), polystyrene (PS), poly(ethylene terephthalate) (PET), and polyvinyl chloride (PVC), into CNMs such as carbon spheres (CSs), carbon nanotubes (CNTs), cup-stacked CNTs (CS-CNTs), carbon nanofibers (CNFs), and
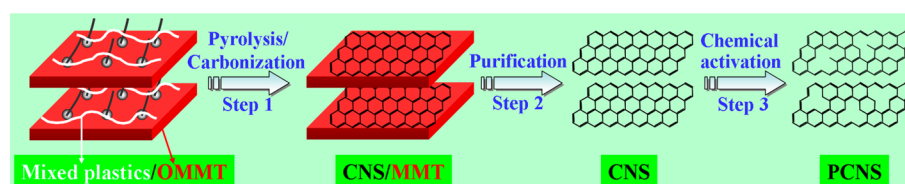
Figure 1. Schematic illustration showing the process of synthesizing PCNS from mixed plastics.

hollow CSs (HCSs). For example, Sawant et al. used autoclave to convert PP, PE, and polyacrylate into CSs, which were used as templates to prepare nanocrystalline CuO hollow spheres.[22] Wu et al. catalyzed gasification of waste PP, PE, and PS into CNTs with hydrogen-rich synthesis gas using a Ni−Mn−Al catalyst.[24] Acomb et al. used pyrolysis−gasification of PP, PE, and PS to prepare CNTs and hydrogen using a Ni/Al$_2$O$_3$ catalyst.[26] Zhuo et al. synthesized CNTs from recycled PE using stainless steel wire mesh as the catalyst using a novel pyrolysis−combustion technique.[27] Very recently, they found that oxidative heat treatment of stainless steel is favored for production of CNTs.[29] Pol et al. used autoclave as the reactor to transform PE into CNTs and CSs, which showed high performances in lithium electrochemical cells.[30] Ruan et al. converted waste PS into high quality graphene using a Cu foil as the template by chemical vapor deposition.[33] Our group found that the combination of solid acid such as HZSM-5 (or halogenated compounds such as CuCl or activated carbon) with a nickel (or cobalt) catalyst could catalyze carbonization of PP, PE, and PS into CNTs, CS-CNTs, CNFs, and HCSs with high yield under atmospheric conditions.[34−40]

Unfortunately, most of current studies are limited to single component plastic, and no studies involving mixed plastics consisting of PP, PE, PS, PET, and PVC, which represent the main composition of "real world" waste plastics,[41] have been reported to date. Thereby, converting mixed plastics into valuable CNMs with controlled morphology is essential for comprehensive utilization of the large amount of "real world" waste plastics. Besides, despite the great efforts to transform plastics into CNMs with various morphologies,[20−40] little attention has been paid to carbon nanosheets (CNS), which show a two-dimensional carbon nanostructure of stacked graphene sheets a few nanometers thickness. CNS have recently been a hot topic owing to their high surface area, developed porous structure, low density, abundant functional groups, and good stability, and their potential applicability in various fields such as adsorption,[42] energy storage,[43] organic transistor,[44] oxygen reduction reaction,[45] etc. A great many of the carbon sources have been used for the synthesis of CNS, for example, hexachloroethane,[42] polyaniline,[43] pitch,[44,46] folic acid,[45] methane,[47,48] ladder-like compounds,[49] phenol-form-aldehyde resin,[50] resorcinol−formaldehyde resin,[51−53] and acetylene.[54] Various methods have been developed to prepare CNS such as solid-state dechlorination,[42] pyrolysis,[43−46,49−53] and plasma-enhanced chemical vapor deposition.[48,54] However, most of these methods usually need a long time for preparation, organic solvents, sophisticated procedures, expensive or toxic precursors, and/or vacuum systems, which limit their applications. Consequently, the development of environ-mentally friendly and cost-effective methods is highly desirable for the large-scale production and application of CNS. More importantly, from the sustainable view, converting mixed plastics into CNS not only shows advantages with cheap and abundant sources, and environmentally friendly and cost-

effective methods, but also provides a novel sustainable approach to recycle waste plastics and relieves the ever-increasing serious energy crisis.

In this work, mixed plastics consisting of PP, PE, PS, PET, and PVC were effectively transformed into CNS on organically modified montmorillonite (OMMT). After KOH activation, porous CNS (PCNS) were prepared. The morphology, microstructure, textural property, phase structure, surface element composition and thermal stability of PCNS were investigated. It was found that PCNS exhibited high specific surface area (1734 m^2/g) and large pore volume (2.441 cm^3/g). More importantly, PCNS were demonstrated to show high performances in the uptake of carbon dioxide and storage of hydrogen.

■ EXPERIMENTAL SECTION

Materials. Polypropylene (PP, trademark T30S) powder was supplied by Yanan Petrochemical Co., China. Polyethylene (PE, trademark 5306J) pellets were obtained from Sinopec Yangzi Petrochemical Co., Ltd., China. Polystyrene (PS, trademark PG-383) pellets were supplied by Zhenjiang Qimei Chemical Co., Ltd., China. Poly(ethylene terephthalate) (PET, trademark SB500) pellets were provided by Sinopec Yizheng Chemical Fiber Co., Ltd., China. Polyvinyl chloride (PVC, trademark PVC1000) powder was obtained from LG Dagu Chemical Ltd., Tianjin, China. Organically modified montmorillonite (OMMT, trademark Closite 15A, organic modifier: dimethyl-dihydrogenated tallow quarternary ammonium, and modifier concentration of 125 mequiv per 100 g of clay) was purchased from Southern Clay. Commercially activated carbon (AC, trademark DTO, specific surface area = 1026 m^2/g, total pore volume = 0.6307 cm^3/g, and micropore volume = 0.4112 cm^3/g) was supplied by Gryfscand, Poland, and used as the reference sample. All other chemicals were of analytical-grade quality.

Preparation of PCNS. Mixed plastics (10.00 g) consisting of PP (35 wt %, 3.50 g), PE (40 wt %, 4.00 g), PS (18 wt %, 1.80 g), PET (4 wt %, 0.40 g), and PVC (3 wt %, 0.30 g) according to previous work[41] were mixed with OMMT at a weight ratio of 1:5 in a Brabender mixer at 100 rpm and 190 °C for 5 min. The CNS/MMT composite was then synthesized by carbonizing the resultant mixed plastics/OMMT composite (Figure 1, step 1) in a conventional quartz tube reactor with an internal diameter of 60 mm at 700 °C for 10 min under a N$_2$ atmosphere (Figure S1, Supporting Information). Our previous work demonstrated that OMMT not only promoted the degradation of mixed plastics into aromatics and light hydrocarbons, but also catalyzed these degradation products into CNS via polymerization mechanism.[55] This is because the OMMT crystal structure consists of stacked layers made of two silica tetrahedrons fused to an edge-shared octahedral sheet of alumina; therefore, OMMT can be used as the template for the growth of CNS. That is to say, OMMT acts as both template and catalyst for synthesis of CNS. Subsequently, after purifying the CNS/MMT composite with hydrofluoric acid and nitric acid (Figure 1, step 2), 6.09 g of CNS was obtained and then mixed with KOH at a weight ratio of 1:6 and chemically activated at 850 °C for 1.5 h under an Ar atmosphere. The resultant mixture was washed with 15 wt % HCl solution and then deionized water to a neutral condition and was finally dried at 120 °C for 12 h (Figure 1, step 3) to produce PCNS (3.77 g).

Characterization. The morphologies of CNS and PCNS were observed by field-emission scanning electron microscopy (FE-SEM, XL30ESEM-FEG). The microstructures of CNS and PCNS were investigated using transmission electron microscopy (TEM, JEM-1011) at an accelerating voltage of 100 kV and high-resolution TEM (HRTEM) on a FEI Tecnai G2 S-Twin transmission electron microscope operating at 200 kV. The textural properties of CNS and PCNS were measured by nitrogen adsorption/desorption at 77 K using a Quantachrome Autosorb-1C-MS analyzer. The specific surface area was calculated by the Brunauer−Emmett−Teller (BET) method. The phase structures of CNS and PCNS were analyzed by X-ray diffraction (XRD) using a D8 advance X-ray diffractometer with Cu Kα radiation operating at 40 kV and 200 mA. Raman spectroscopy (T6400, excitation beam wavelength = 514.5 nm) was used to characterize the vibrational properties of CNS and PCNS. The surface element compositions of CNS and PCNS were characterized by means of X-ray photoelectron spectroscopy (XPS) carried out on a VG ESCALAB MK II spectrometer using an Al Kα exciting radiation from an X-ray source operated at 10.0 kV and 10 mA. The thermal stabilities of CNS and PCNS were measured by thermal gravimetric analysis (TGA) under air flow at a heating rate of 10 °C/min using a TA Instruments SDT Q600. Adsorption capacities of carbon dioxide and hydrogen were measured using a Sievert-type volumetric apparatus (IMI, Hiden Isochema, U.K.).

RESULTS AND DISCUSSION

Morphology and Microstructure. The morphology and microstructure of CNS and PCNS are characterized by FE-SEM, TEM, and HRTEM observations. As shown in Figure 2a
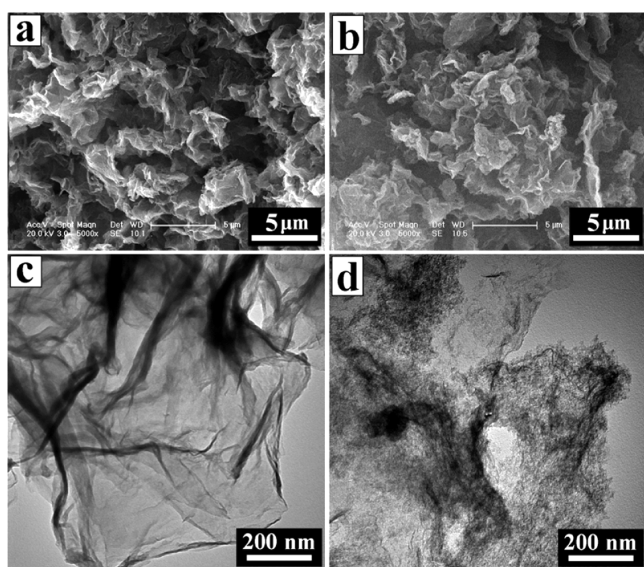

Figure 2. FE-SEM and TEM images of CNS (a, c) and PCNS (b, d).

and b, CNS and PCNS displayed layered morphology and consisted of thin leaf-like agglomerated nanosheets ranging from hundreds of nanometers to several micrometers in length. TEM analysis demonstrated the sheet-like arrangement of CNS with randomly arranged a wrinkled structure and rough surface (Figure 2c). Comparatively, PCNS still maintained a crumbled thin sheet structure, but the surface of PCNS became obviously rougher than that of CNS (Figure 2d). HRTEM images of CNS revealed a negligible degree of ordering (Figure 3a and b), which indicated its low graphitization degree. After KOH activation, a lot of micropores and mesopores were observed in PCNS (Figure 3c), similar to porous graphene activated by KOH as reported previously.[56] This result demonstrated that
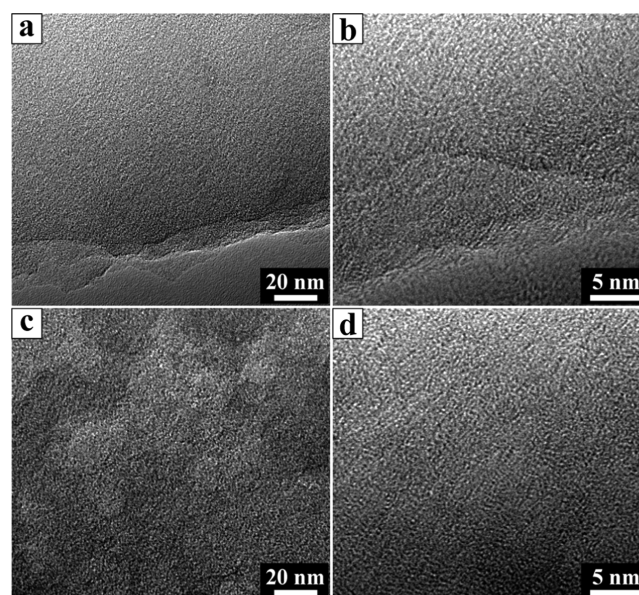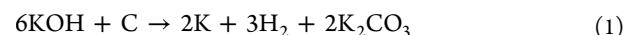

Figure 3. HRTEM images of CNS (a, b) and PCNS (c, d).

the KOH activation process was able to etch graphitic layers to form a porous structure. The activation mechanism is normally suggested to include independent hydroxide and redox processes during the reaction.[57] With the activation treatment, KOH powder can react with carbon as follows

$$6KOH + C \rightarrow 2K + 3H_2 + 2K_2CO_3 \qquad (1)$$

When the temperature is higher than 700 °C, the reaction proceeds as follows

$$K_2CO_3 + C \leftrightarrow K_2O + 2CO \qquad (2)$$

$$K_2CO_3 \leftrightarrow K_2O + CO_2 \qquad (3)$$

$$2K + CO_2 \leftrightarrow K_2O + CO \qquad (4)$$

When the temperature is higher than 800 °C, the reaction proceeds as follows

$$K_2O + C \leftrightarrow 2K + CO \qquad (5)$$

Textural Property, Phase Structure, Surface Element Composition, and Thermal Stability. Nitrogen adsorption/desorption experiments are carried out at 77 K to characterize the porosity of CNS and PCNS. Evidently, PCNS exhibited the combined type I/IV physisorption isotherm (Figure 4a). A high adsorption capacity was observed at low relative pressure (P/P_0 < 0.1), which indicated the presence of many micropores. The type-H4 hysteresis loop at a relative pressure P/P_0 ranging from 0.4 to 1.0, which resulted from the filling and emptying of the mesopores by capillary condensation, suggested the generation of a large number of mesopores. PCNS were found to show high specific surface area (S_{BET}) of 1734.0 m²/g and large pore volume (V) of 2.441 cm³/g, in comparison to CNS (S_{BET} = 128.9 m²/g and V = 0.667 cm³/g). The remarkable S_{BET} and V_{total} enhancements were ascribed to KOH-activated treatment, which is a very efficient method to etch pores and increase the content of defective and edge sites. In addition, PCNS mainly displayed significant mesoporosity with a narrow pore size distribution centered at about 3.8 nm (Figure 4b), which was consistent with the HRTEM result. The pores could be attributed to the cavities in the PCNS.
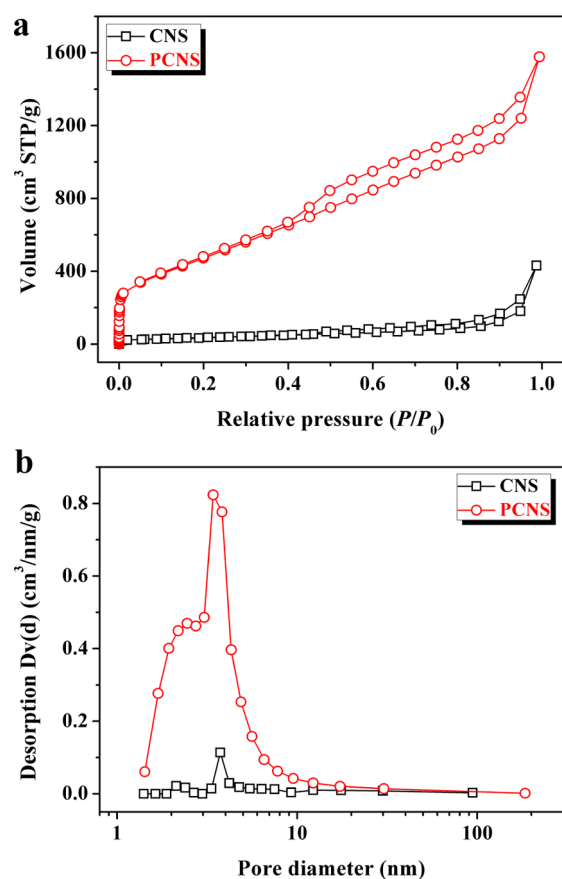
Figure 4. Nitrogen adsorption/desorption isotherms (a) and pore size distributions (b) of CNS and PCNS.

Figure 5. XRD patterns (a) and Raman spectra (b) of CNS and PCNS.

XRD and Raman measurements are employed to investigate the phase structures of CNS and PCNS. The appearance of two weak and broad diffraction peaks at $2\theta = 26.2°$ and $43.3°$ (Figure 5a), assigned to the typical graphitic (002) and (101) planes, respectively,[58] indicated the low degree of graphitization of CNS. The absence of the (002) characteristic peak of pristine graphite reflected the disordered nature and irregular arrangement of carbon layers in the resultant PCNS, which was in good agreement with HRTEM observation. The D band at about 1339 cm^{-1} and G band at about 1585 cm^{-1} in the Raman spectra of CNS and PCNS (Figure 5b) are related to the disordered and defective structure of the carbon material and ordered carbon structure with sp^2 electronic configuration, respectively.[59] It is well known that the intensity ratio of G/D peak (I_G/I_D) is often used to estimate the degree of perfection of graphene planes.[60,61] The I_G/I_D value decreased from 0.61 for CNS to 0.48 for PCNS, which was mainly ascribed to the generation of a great number of defects by KOH activation. In addition, the negligible 2D band at about 2670 cm^{-1} and D + G band at about 2920 cm^{-1} verified the amorphous nature and multilayers of both CNS and PCNS.[62]

XPS is conducted to characterize the surface element compositions of CNS and PCNS. It revealed that the surfaces of CNS and PCNS were composed of C (284.6 eV) and O (531.9 eV) elements with no evidence of any other elements (Figure S2, Supporting Information). To determine the chemical component and oxidation state of the C element, high-resolution XPS spectra of C 1s are curve-fitted into four individual peaks: graphitic carbon (284.4–284.6 eV), −C−OH (285.6–285.7 eV), −C═O (286.7–287.0 eV), and −COOH
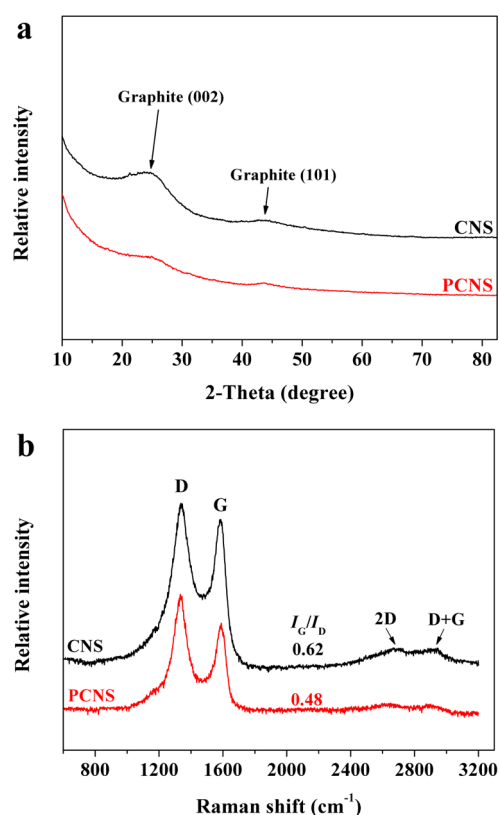
(288.7−289.0 eV), as shown in Figure 6. Comparing with CNS, PCNS possessed a relatively higher oxygen content and more oxygen-containing surface functional groups including −C−OH, −C═O, and −COOH. TGA and derivative TGA (DTG) are used to evaluate the graphitic nature and purity of CNS and PCNS (Figure 7). The first weak region of weight loss from 100 to 400 °C was attributed to the release of chemisorbed water and the pyrolysis of oxygen-containing functional groups. A remarkable weight loss occurred between 400 and 800 °C, which was ascribed to the oxidation of the carbon skeleton of graphene sheets. The lower maximum oxidation temperature of PCNS (530.9 °C) than that of CNS (583.8 °C) demonstrated the formation of a lot of defects and/or oxygen-containing functional groups by KOH activation. The residues of CNS and PCNS at 800 °C were calculated to be less than 0.5 wt %, indicating that both CNS and PCNS have high purity.

Uptake of Carbon Dioxide and Storage of Hydrogen. In our modern society, the mitigation of CO_2 emission is a crucial issue because this gas is the main anthropogenic contributor to climate change. Among the possible strategies for CO_2 abatement, capture and storage have attracted keen interest.[7,52] Carbon materials have been widely investigated in CO_2 uptake in terms of their being lightweight and having low cost and unique chemical and physical properties.[42] On the other hand, hydrogen with the advantages of abundance, high energy density, and environmental friendliness is one of the most promising future sustainable energy fuels to reduce the dependence on fossil fuels and their associated environmental impact.[63,64] Hydrogen storage is currently one of the main obstacles hindering the commercial use of hydrogen. Among the large variety of materials investigated as carriers for hydrogen storage, porous carbons have generated a great deal
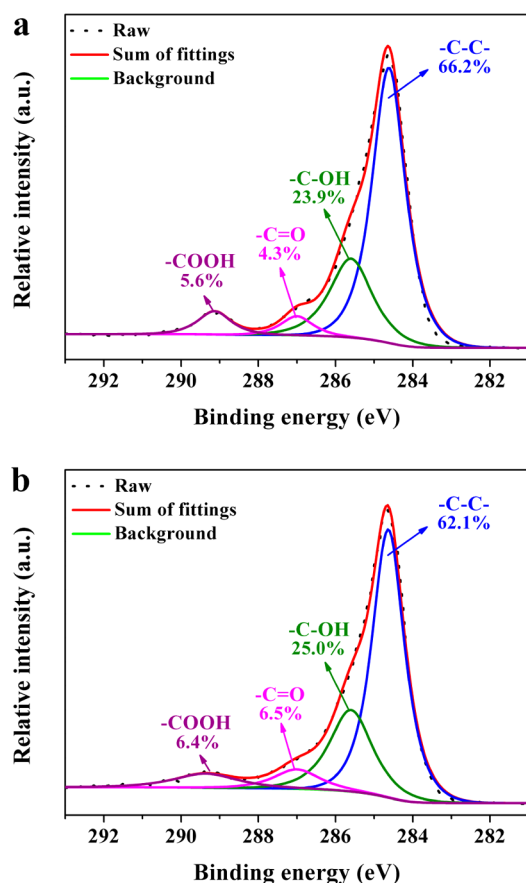
Figure 6. C 1s high-resolution XPS spectra of CNS (a) and PCNS (b).

Figure 7. TGA (a) and DTG (b) curves of CNS and PCNS under air flow at 10 °C/min.

of attention,[65] but the preparation of porous carbons with high hydrogen adsorption capacity still remains a great challenge for practical applications.

Figure 8a shows the CO_2 adsorption isotherms for CNS and PCNS at 313 K using a volumetric technique. For both CNS and PCNS, the CO_2 uptake capacity increased with increasing CO_2 pressure, which is indicative of the typical physisorption behavior. Remarkably, PCNS showed higher CO_2 uptake capacity than CNS. For example, at the pressures of 10 and 45 bar, the CO_2 uptake capacity of PCNS was measured to be 6.75 and 18.00 mmol/g, respectively, which was about 4.8 and 5.9 times as that of CNS, respectively. Figure 8b shows the hydrogen adsorption isotherms for CNS and PCNS at 313 K. It was observed that the hydrogen adsorption capacity for CNS and PCNS increased with increasing hydrogen pressure. The adsorption capacity of PCNS could reach up to 3.0 and 5.2 mmol/g at the hydrogen pressures of 25 and 45 bar, respectively, while CNS showed adsorption capacity of 0.9 and 1.4 mmol/g, respectively. More importantly, the hydrogen adsorption capacity of PCNS is higher than that of many other carbon materials. For example, Wenelska et al. recently synthesized Pd nanoparticle-supported hollow carbon spheres, of which the maximum hydrogen capacity was calculated to be 1.8 mmol/g at a hydrogen pressure of 25 bar.[66] Besides, the hydrogen capacity of PCNS at a hydrogen pressure of 45 bar is about 8.6 times as much as that of commercial AC (0.6 mmol/g).

Overall, PCNS were considerably more effective in the uptake of carbon dioxide and storage of hydrogen than CNS, which was obvi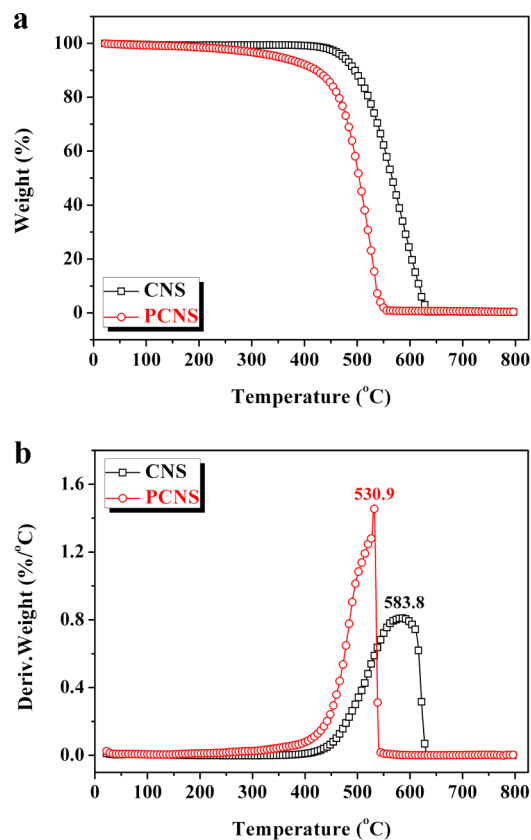ously ascribed to the existence of plenty of micropores and mesopores originated from KOH activation (Figure 4). Future work to adjust the porous structure of PCNS and further improve their performances in the uptake of carbon dioxide and storage of hydrogen is on the way. Nevertheless, the synthesized PCNS with simplicity, high performance, low cost in operation, and easy availability of raw materials could be considered a promising candidate for environment remediation and energy storage, etc.

■ CONCLUSIONS

A novel, facile, and sustainable approach was established to convert mixed plastics consisting of PP, PE, PS, PET, and PVC into high value-added PCNS. According to FE-SEM, TEM, and HRTEM observations, PCNS contained randomly oriented lattice fringes and showed a layered morphology consisting of thin, leaf-like, agglomerated nanosheets ranging from hundreds of nanometers to several micrometers in length. Besides, PCNS exhibited high specific surface area (1734 m^2/g) and large pore volume (2.441 cm^3/g) with high purity (more than 99.5%). More importantly, PCNS were demonstrated to show high performances in the uptake of carbon dioxide and storage of hydrogen. In addition, it is worth noting that the degradation products of mixed plastics such as hydrogen, propylene, and benzene during the growth of CNS could be used as important chemicals and fuels. It is believed that this work will not only pave the way for large-scale utilization of mixed waste plastics but also advance the sustainable production of valuable PCNS for various applications such as energy storage, environmental remediation, catalysis, etc. Related investigations are being conducted in our laboratory.
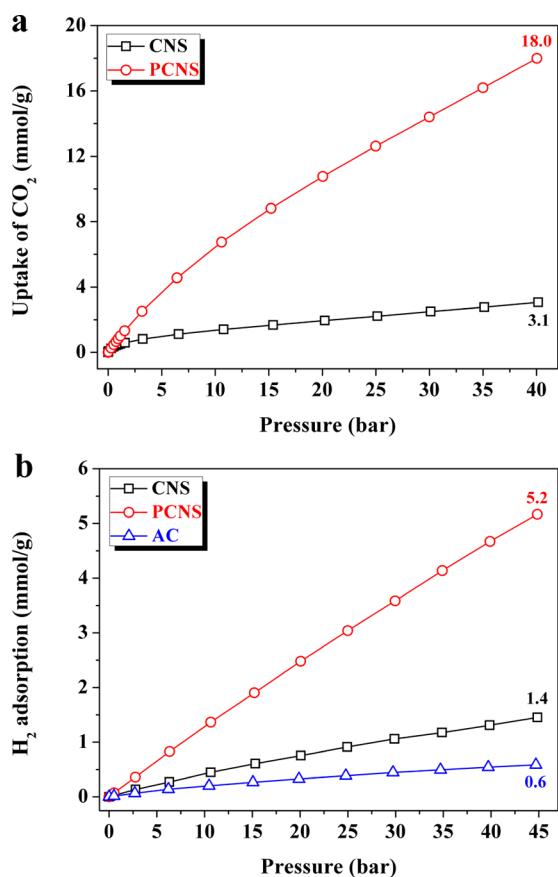
Figure 8. Carbon dioxide (a) and hydrogen (b) adsorption isotherms for CNS, PCNS, and AC at 313 K.

■ ASSOCIATED CONTENT

Ⓢ Supporting Information

Schematic diagram of carbonization of the mixed plastics/OMMT composite (Figure S1) and XPS spectra of CNS and PCNS (Figure S2). This material is available free of charge via the Internet at http://pubs.acs.org.

■ AUTHOR INFORMATION

Corresponding Authors
*Tel: +86 (0) 431 85262004. Fax: +86 (0) 431 85262827. E-mail: xchen@ciac.ac.cn (X.C.).
*Tel: +86 (0) 431 85262004. Fax: +86 (0) 431 85262827. E-mail: ttang@ciac.ac.cn (T.T.).

Notes

The authors declare no competing financial interest.

■ ACKNOWLEDGMENTS

■ REFERENCES

(1) Titirici, M. M.; Antonietti, M. Chemistry and materials options of sustainable carbon materials made by hydrothermal carbonization. *Chem. Soc. Rev.* **2010**, *39*, 103−116.

(2) Galhardo, T. S.; Simone, N.; Gonçalves, M.; Figueiredo, F. C. A.; Mandelli, D.; Carvalho, W. A. Preparation of sulfonated carbons from rice husk and their application in catalytic conversion of glycerol. *ACS Sustainable Chem. Eng.* **2013**, *1*, 1381−1389.

(3) Li, Y. Q.; Samad, Y. A.; Polychronopoulou, K.; Alhassan, S. M.; Liao, K. Carbon aerogel from winter melon for highly efficient and recyclable oils and organic solvents absorption. *ACS Sustainable Chem. Eng.* **2014**, *2*, 1492−1497.

(4) Nagarajan, V.; Mohanty, A. K.; Misra, M. Sustainable green composites: Value addition to agricultural residues and perennial grasses. *ACS Sustainable Chem. Eng.* **2013**, *1*, 325−333.

(5) Wu, C. F.; Wang, L. Z.; Williams, P. T.; Shi, J.; Huang, J. Hydrogen production from biomass gasification with Ni/MCM-41 catalysts: Influence of Ni content. *Appl. Catal., B* **2011**, *108−109*, 6−13.

(6) Xu, Q.; Qian, Q. F.; Quek, A.; Ai, N.; Zeng, G. N.; Wang, J. W. Hydrothermal carbonization of macroalgae and the effects of experimental parameters on the properties of hydrochars. *ACS Sustainable Chem. Eng.* **2013**, *1*, 1092−1101.

(7) Titirici, M. M.; White, R. J.; Falco, C.; Sevilla, M. Black perspectives for a green future: Hydrothermal carbons for environment protection and energy storage. *Energy Environ. Sci.* **2012**, *5*, 6796−6822.

(8) Sarawade, P.; Tan, H.; Polshettiwar, V. Shape- and morphology-controlled sustainable synthesis of Cu, Co, and in metal organic frameworks with high CO₂ capture capacity. *ACS Sustainable Chem. Eng.* **2013**, *1*, 66−74.

(9) Sacia, E. R.; Ramkumar, S.; Phalak, N.; Fan, L. S. Synthesis and regeneration of sustainable CaO sorbents from chicken eggshells for enhanced carbon dioxide capture. *ACS Sustainable Chem. Eng.* **2013**, *1*, 903−909.

(10) Hassan, T. A.; Rangari, V. K.; Jeelani, S. Value-added biopolymer nanocomposites from waste eggshell-based CaCO₃ nanoparticles as fillers. *ACS Sustainable Chem. Eng.* **2014**, *2*, 706−717.

(11) Hu, C.; Yu, C.; Li, M. Y.; Fan, X. M.; Yang, J.; Zhang, P.; Wang, S. Y.; Zhao, Z. B.; Qiu, J. S. Preparation of single-walled carbon nanotubes from fullerene waste soot. *ACS Sustainable Chem. Eng.* **2014**, *2*, 14−18.

(12) Sengupta, S.; Ray, D.; Mukhopadhyay, A. Sustainable materials: Value-added composites from recycled polypropylene and fly ash using a green coupling agent. *ACS Sustainable Chem. Eng.* **2013**, *1*, 574−584.

(13) Hu, S. X.; Hsieh, Y. L. Preparation of activated carbon and silica particles from rice straw. *ACS Sustainable Chem. Eng.* **2014**, *2*, 726−734.

(14) *Plastics—The Facts 2013: An Analysis of European Latest Plastics Production, Demand and Waste Data*; PlasticsEurope, Brussels, 2013.

(15) Municipal Solid Waste Generation, Recycling, and Disposal in the United States: Facts and Figures for 2012; U.S. Environmental Protection Agency: Washington DC, 2012.

(16) Dorado, C.; Mullen, C. A.; Boateng, A. A. H-ZSM5 catalyzed co-pyrolysis of biomass and plastics. *ACS Sustainable Chem. Eng.* **2014**, *2*, 301−311.

(17) Williams, P. T.; Slaney, E. Analysis of products from the pyrolysis and liquefaction of single plastics and waste plastic mixtures. *Resour. Conserv. Recycl.* **2007**, *51*, 754−769.

(18) Al-Salem, S. M.; Lettieri, P.; Baeyens, J. Recycling and recovery routes of plastic solid waste (PSW): A review. *Waste Manage.* **2009**, *29*, 2625−2643.

(19) Serrano, D. P.; Aguado, J.; Escola, J. M. Developing advanced catalysts for the conversion of polyolefinic waste plastics into fuels and chemicals. *ACS Catal.* **2012**, *2*, 1924−1941.

(20) Bazargan, A.; McKay, G. A review—Synthesis of carbon nanotubes from plastic wastes. *Chem. Eng. J.* **2012**, *195−196*, 377−391.

(21) Zhuo, C. W.; Levendis, Y. A. Upcycling waste plastics into carbon nanomaterials: A review. *J. Appl. Polym. Sci.* **2014**, *131*, 39931−39944.

(22) Sawant, S. Y.; Somani, R. S.; Panda, A. B.; Bajaj, H. C. Utilization of plastic wastes for synthesis of carbon microspheres and their use as a template for nanocrystalline copper(II) oxide hollow spheres. *ACS Sustainable Chem. Eng.* **2013**, *1*, 1390−1397.

(23) Sawant, S. Y.; Somani, R. S.; Panda, A. B.; Bajaj, H. C. Formation and characterization of onions shaped carbon soot from plastic wastes. *Mater. Lett.* **2013**, *94*, 132−135.

(24) Wu, C. F.; Nahil, M. A.; Miskolczi, N.; Huang, J.; Williams, P. T. Processing real-world waste plastics by pyrolysis-reforming for hydrogen and high-value carbon nanotubes. *Environ. Sci. Technol.* **2014**, *48*, 819−826.

(25) Wu, C. F.; Wang, Z. C.; Wang, L. Z.; Williams, P. T.; Huang, J. Sustainable processing of waste plastics to produce high yield hydrogen-rich synthesis gas and high quality carbon nanotubes. *RSC Adv.* **2012**, *2*, 4045−4047.

(26) Acomb, J. C.; Wu, C. F.; Williams, P. T. Control of steam input to the pyrolysis-gasification of waste plastics for improved production of hydrogen or carbon nanotubes. *Appl. Catal., B* **2014**, *147*, 571−584.

(27) Zhuo, C. W.; Hall, B.; Richter, H.; Levendis, Y. Synthesis of carbon nanotubes by sequential pyrolysis and combustion of polyethylene. *Carbon* **2010**, *48*, 4024−4034.

(28) Zhuo, C. W.; Alves, J. O.; Tenorio, J. A. S.; Levendis, Y. A. Synthesis of carbon nanomaterials through up-cycling agricultural and municipal solid wastes. *Ind. Eng. Chem. Res.* **2012**, *51*, 2922−2930.

(29) Zhuo, C. W.; Wang, X.; Nowak, W.; Levendis, Y. A. Oxidative heat treatment of 316L stainless steel for effective catalytic growth of carbon nanotubes. *Appl. Surf. Sci.* **2014**, *313*, 227−236.

(30) Pol, V. G.; Thackeray, M. M. Spherical carbon particles and carbon nanotubes prepared by autogenic reactions: Evaluation as anodes in lithium electrochemical cells. *Energy Environ. Sci.* **2011**, *4*, 1904−1912.

(31) Pol, V. G. Upcycling: Converting waste plastics into paramagnetic, conducting, solid, pure carbon microspheres. *Environ. Sci. Technol.* **2010**, *44*, 4753−4759.

(32) Wei, L. Z.; Yan, N.; Chen, Q. W. Converting poly(ethylene terephthalate) waste into carbon microspheres in a supercritical CO_2 system. *Environ. Sci. Technol.* **2011**, *45* (2), 534−539.

(33) Ruan, G. D.; Sun, Z. Z.; Peng, Z. W.; Tour, J. M. Growth of graphene from food, insects, and waste. *ACS Nano* **2011**, *5* (9), 7601−7607.

(34) Tang, T.; Chen, X. C.; Meng, X. Y.; Chen, H.; Ding, Y. P. Synthesis of multiwalled carbon nanotubes by catalytic combustion of polypropylene. *Angew. Chem., Int. Ed.* **2005**, *44*, 1517−1520.

(35) Jiang, Z. W.; Song, R. J.; Bi, W. G.; Lu, J.; Tang, T. Polypropylene as a carbon source for the synthesis of multi-walled carbon nanotubes via catalytic combustion. *Carbon* **2007**, *45*, 449−458.

(36) Song, R. J.; Jiang, Z. W.; Bi, W. G.; Cheng, W. X.; Lu, J.; Huang, B. T.; Tang, T. The combined catalytic action of solid acids with nickel for the transformation of polypropylene into carbon nanotubes by pyrolysis. *Chem.—Eur. J.* **2007**, *13*, 3234−3240.

(37) Gong, J.; Liu, J.; Ma, L.; Wen, X.; Chen, X. C.; Wan, D.; Yu, H. O.; Jiang, Z. W.; Borowiak-Palen, E.; Tang, T. Effect of Cl/Ni molar ratio on the catalytic conversion of polypropylene into Cu−Ni/C composites and their application in catalyzing "click" reaction. *Appl. Catal., B* **2012**, *117–118*, 185−193.

(38) Gong, J.; Liu, J.; Wan, D.; Chen, X. C.; Wen, X.; Mijowska, E.; Jiang, Z. W.; Wang, Y. H.; Tang, T. Catalytic carbonization of polypropylene by the combined catalysis of activated carbon with Ni_2O_3 into carbon nanotubes and its mechanism. *Appl. Catal., A* **2012**, *449*, 112−120.

(39) Gong, J.; Liu, J.; Jiang, Z. W.; Feng, J. D.; Chen, X. C.; Wang, L.; Mijowska, E.; Wen, X.; Tang, T. Striking influence of chain structure of polyethylene on the formation of cup-stacked carbon nanotubes/carbon nanofibers under the combined catalysis of CuBr and NiO. *Appl. Catal., B* **2014**, *147*, 592−601.

(40) Gong, J.; Liu, J.; Jiang, Z. W.; Chen, X. C.; Wen, X.; Mijowska, E.; Tang, T. Converting mixed plastics into mesoporous hollow carbon spheres with controllable diameter. *Appl. Catal., B* **2014**, *152–153*, 289−299.

(41) López, A.; de Marco, I.; Caballero, B. M.; Laresgoiti, M. F.; Adrados, A.; Aranzabal, A. Catalytic Pyrolysis of plastic wastes with two different types of catalysts: ZSM-5 zeolite and red mud. *Appl. Catal., B* **2011**, *104*, 211−219.

(42) Sawant, S. Y.; Somani, R. S.; Sharma, S. S.; Bajaj, H. C. Solid-state dechlorination pathway for the synthesis of few layered functionalized carbon nanosheets and their greenhouse gas adsorptivity over CO and N_2. *Carbon* **2014**, *68*, 2100−2200.

(43) Wen, Q.; Wang, S. Y.; Yan, J.; Cong, L. J.; Chen, Y.; Xi, H. Y. Porous nitrogen-doped carbon nanosheet on graphene as metal-free catalyst for oxygen reduction reaction in air-cathode microbial fuel cells. *Bioelectrochemistry* **2014**, *95*, 23−28.

(44) Lee, J. S.; Joh, H. I.; Kim, T. W.; Lee, S. Carbon nanosheets derived from soluble pitch molecules and their applications in organic transistors. *Org. Electron.* **2014**, *15*, 132−138.

(45) Wang, Y. C.; Jiang, X. E. Facile preparation of porous carbon nanosheets without template and their excellent electrocatalytic property. *ACS Appl. Mater. Interfaces* **2013**, *5*, 11597−11602.

(46) Fan, Z. J.; Liu, Y.; Yan, J.; Ning, G. Q.; Wang, Q.; Wei, T.; Zhi, L. J.; Wei, F. Template-directed synthesis of pillared-porous carbon nanosheet architectures: High-performance electrode materials for supercapacitors. *Adv. Energy Mater.* **2012**, *2*, 419−424.

(47) Wang, Z. P.; Shoji, M.; Ogata, H. Carbon nanosheets by microwave plasma enhanced chemical vapor deposition in CH_4−Ar system. *Appl. Surf. Sci.* **2011**, *257*, 9082−9085.

(48) Zhao, X.; Tian, H.; Zhu, M. Y.; Tian, K.; Wang, J. J.; Kang, F. Y.; Outlaw, R. A. Carbon nanosheets as the electrode material in supercapacitors. *J. Power Sources* **2009**, *194*, 1208−1212.

(49) Son, S. Y.; Noh, Y. J.; Bok, C.; Lee, S.; Kim, B. G.; Na, S. I.; Joh, H. I. One-step synthesis of carbon nanosheets converted from a polycyclic compound and their direct use as transparent electrodes of ITO-free organic solar cells. *Nanoscale* **2014**, *6*, 678−682.

(50) Fang, Y.; Lv, Y. Y.; Che, R. C.; Wu, H. Y.; Zhang, X. H.; Gu, D.; Zheng, G. F.; Zhao, D. Y. Two-dimensional mesoporous carbon nanosheets and their derived graphene nanosheets: Synthesis and efficient lithium ion storage. *J. Am. Chem. Soc.* **2013**, *135*, 1524−1530.

(51) Zhang, J. T.; Jin, Z. Y.; Li, W. C.; Dong, W.; Lu, A. H. Graphene modified carbon nanosheets for electrochemical detection of Pb(II) in water. *J. Mater. Chem. A* **2013**, *1*, 13139−13145.

(52) Hao, G. P.; Jin, Z. Y.; Sun, Q.; Zhang, X. Q.; Zhang, J. T.; Lu, A. H. Porous carbon nanosheets with precisely tunable thickness and selective CO_2 adsorption properties. *Energy Environ. Sci.* **2013**, *6*, 3740−3747.

(53) Jin, Z. Y.; Lu, A. H.; Xu, Y. Y.; Zhang, J. T.; Li, W. C. Ionic liquid-assisted synthesis of microporous carbon nanosheets for use in high rate and long cycle life supercapacitors. *Adv. Mater.* **2014**, *26* (22), 3700−3705.

(54) Cott, D. J.; Verheijen, M.; Richard, O.; Radu, I.; Gendt, S. D.; Elshocht, van S.; Vereecken, P. M. Synthesis of large area carbon nanosheets for energy storage applications. *Carbon* **2013**, *58*, 59−65.

(55) Gong, J.; Liu, J.; Wen, X.; Jiang, Z. W.; Chen, X. C.; Mijowska, E.; Tang, T. Upcycling waste polypropylene into graphene flakes on organically modified montmorillonite. *Ind. Eng. Chem. Res.* **2014**, *53*, 4173−4181.

(56) Zhu, Y.; Murali, S.; Stoller, M. D.; Ganesh, K. J.; Cai, W.; Ferreira, P. J.; Pirkle, A.; Wallace, R. M.; Cychosz, K. A.; Thommes, M.; Su, D.; Stach, E. A.; Ruoff, R. S. Carbon-based supercapacitors produced by activation of graphene. *Science* **2011**, *332*, 1537−1541.

(57) Wang, J. C.; Kaskel, S. KOH activation of carbon-based materials for energy storage. *J. Mater. Chem.* **2012**, *22*, 23710−23725.

(58) Gong, J.; Feng, J. D.; Liu, J.; Jiang, Z. W.; Chen, X. C.; Mijowska, E.; Wen, X.; Tang, T. Catalytic carbonization of polypropylene into cup-stacked carbon nanotubes with high performances in adsorption of heavy metallic ions and organic dyes. *Chem. Eng. J.* **2014**, *248*, 27−40.

(59) Gupta, S. S.; Sreeprasad, T. S.; Maliyekkal, S. M.; Das, S. K.; Pradeep, T. Graphene from sugar and its application in water purification. *ACS Appl. Mater. Interfaces* **2012**, *4*, 4156−4163.

(60) Wu, C. F.; Dong, L.; Huang, J.; Williams, P. T. Optimising the sustainability of crude bio-oil via reforming to hydrogen and valuable by-product carbon nanotubes. *RSC Adv.* **2013**, *3*, 19239−19242.

(61) Alves, J. O.; Zhuo, C. W.; Levendis, Y. A.; Tenório, J. A. S. Catalytic conversion of wastes from the bioethanol production into carbon nanomaterials. *Appl. Catal., B* **2011**, *106*, 433−444.

(62) John, R.; Ashokreddy, A.; Vijayan, C.; Pradeep, T. Single- and few-layer graphene growth on stainless steel substrates by direct thermal chemical vapor deposition. *Nanotechnology* **2011**, *22*, 165701.

(63) Wu, C. F.; Williams, P. T. Hydrogen production by steam gasification of polypropylene with various nickel catalysts. *Appl. Catal. B: Environ.* **2009**, *87*, 152−161.

(64) Wu, C. F.; Dong, L. S.; Onwudili, J.; Williams, P. T.; Huang, J. Effect of Ni particle location within the mesoporous MCM-41 support for hydrogen production from the catalytic gasification of biomass. *ACS Sustainable Chem. Eng.* **2013**, *1*, 1083−1091.

(65) Chen, J. F.; Lang, Z. L.; Xu, Q.; Hu, B.; Fu, J. W.; Chen, Z. M.; Zhang, J. N. Facile Preparation of monodisperse carbon spheres: Template-free construction and their hydrogen storage properties. *ACS Sustainable Chem. Eng.* **2013**, *1*, 1063−1068.

(66) Wenelska, K.; Michalkiewicz, B.; Gong, J.; Tang, T.; Kaleńczuk, R.; Chen, X. C.; Mijowska, E. In situ deposition of Pd nanoparticles with controllable diameters in hollow carbon spheres for hydrogen storage. *Int. J. Hydrogen Energy* **2013**, *38* (36), 16179−16184.